

## Study of audio speakers containing ferrofluid

This article has been downloaded from IOPscience. Please scroll down to see the full text article.

2008 J. Phys.: Condens. Matter 20 204147

(<http://iopscience.iop.org/0953-8984/20/20/204147>)

View [the table of contents for this issue](#), or go to the [journal homepage](#) for more

Download details:

IP Address: 129.252.86.83

The article was downloaded on 29/05/2010 at 12:02

Please note that [terms and conditions apply](#).

# Study of audio speakers containing ferrofluid

R E Rosensweig<sup>1</sup>, Y Hirota<sup>2</sup>, S Tsuda<sup>2</sup> and K Raj<sup>3</sup>

<sup>1</sup> 34 Gloucester Road, Summit, NJ 07901, USA

<sup>2</sup> Ferrotec, 1-4-14 Kyobashi, chuo-Ku, Tokyo 104-0031, Japan

<sup>3</sup> Ferrotec, 33 Constitution Drive, Bedford, NH 03110, USA

Received 5 April 2008

Published 1 May 2008

Online at [stacks.iop.org/JPhysCM/20/204147](http://stacks.iop.org/JPhysCM/20/204147)

## Abstract

This work validates a method for increasing the radial restoring force on the voice coil in audio speakers containing ferrofluid. In addition, a study is made of factors influencing splash loss of the ferrofluid due to shock. Ferrohydrodynamic analysis is employed throughout to model behavior, and predictions are compared to experimental data.

## 1. Introduction

The use of ferrofluid in audio speakers and the benefits achieved including voice coil cooling and centering are well known [1, 2]. This work examines a proposal for enhancing the centering force by filling just the one gap between the voice coil and the inner pole piece. Experimental limits on the drop height at which fluid loss onsets by splashing is also studied to determine means for increasing ruggedness. Increased shock resistance holds interest also for the use of ferrofluids in seals, instruments, motors, and other devices.

## 2. Analysis of voice coil centering

SI units are employed throughout unless otherwise noted.

The unperturbed geometry of the pole/voice-coil/pole structure of an audio speaker is modeled as three concentric cylinders with the magnetic field radiating symmetrically from the inner pole to the outer one; see figure 1. From Gauss's law the distribution of the induction field magnitude  $B$  is given by  $BR = B_0R_0$  where  $R$  is the radial distance from the center,  $R_0$  the radius of the inner pole piece, and  $B_0$  the induction at  $R = R_0$ . The defining equation is  $B = \mu_0H + M$  expressed in a modified form such that  $M$  carries units of teslas. In the usual high field of an audio gap the magnetization is approximated as saturated,  $M = M_s$ . Thus, magnetic field in the ferrofluid is distributed according to  $\mu_0H = B_0R_0/R - M_s$ .

The net magnitude of force  $F_i$  on the inner surface of the voice coil having wetted length  $L$  when its center undergoes a small displacement is given by

$$F_i = \int_0^{2\pi} p(\theta)\cos(\theta)R_iL d\theta. \quad (1)$$

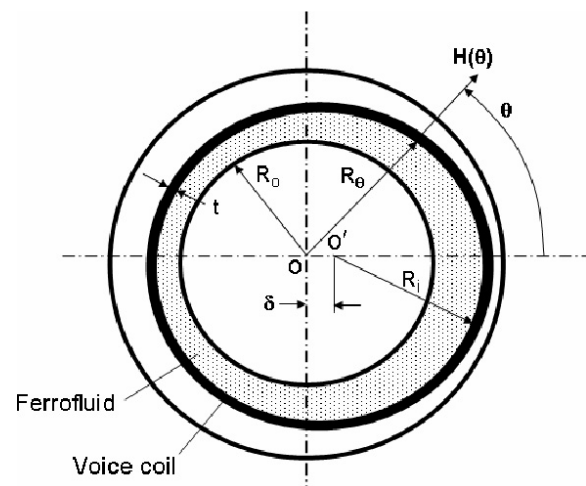


**Figure 1.** Geometry for deriving radial distance  $R(\theta)$  from the center of the inner pole piece having radius  $R_0$  to a point at a position on the voice coil having inner radius  $R_i$ .

Pressure  $p(\theta)$  in a stationary volume of ferrofluid is related to the magnetic field via the ferrohydrodynamic Bernoulli equation [3] with velocity absent and gravity force negligible:

$$p(\theta) - p_0 = \int_{H_0}^{H(\theta)} M dH \quad (2)$$

$p_0$  is pressure at the inner pole surface where the field magnitude is  $H_0$ . For the highly saturated ferrofluid, equation (2) integrates approximately to  $p(\theta) - p_0 = M_s[H(\theta) - H_0]$ . Substituting for  $p(\theta)$  in equation (1) and making the approximation that displacement of the voice coil

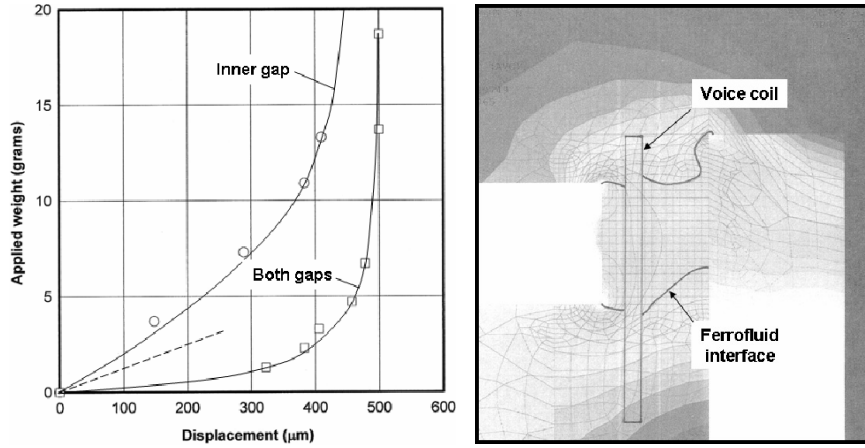


**Figure 2.** Left: comparative displacements of the voice coil in response to a radial force with the fill fraction of 1. The dashed line is the initial slope for a filled inner gap predicted from equation (4). Right: calculated location of ferrofluid interfaces for a fill fraction of 1 in the gaps.

has a small effect on the distribution of the field yields

$$F_i = \frac{B_0 M_s R_0 R_i L}{\mu_0} \int_0^{2\pi} \frac{\cos\theta}{R(\theta)} d\theta. \quad (3)$$

From geometry, the distance  $R(\theta)$  is given by  $R(\theta) = R_i [(\delta/R_i)^2 + 2(\delta/R_i)\cos\theta + 1]^{1/2}$ . For small displacements,  $R(\theta)$  expands to give  $R(\theta) \approx R_i [1 - (\delta/R_i)\cos\theta]^{-1}$ . Substituting this expression into equation (3) and integrating yields the final result for the spring constant  $K_i = F_i/\delta$ :

$$K_i = -\frac{\pi B_0 M_s L}{\mu_0 R_i} R_0 \quad (4)$$

$K_i$  is the contribution to the spring constant due to the ferrofluid pressure force exerted on the inner surface of the displaced voice coil. The minus sign indicates that this contribution to the spring force is restorative.

If only the outer gap is filled with ferrofluid a similar treatment yields the spring constant contribution  $K_o$  due to forces exerted on the outer surface of a thin voice coil having thickness  $t$ :

$$K_o = \frac{\pi B_0 M_s L}{\mu_0 (R_i + t)} R_0. \quad (5)$$

The sign in this case is positive, as the pressure forces at any location are oppositely directed to those acting on the inner surface. The net spring constant when both gaps are filled with ferrofluid is given by  $K = K_i + K_o$ . Substituting from equations (4), and (5) and assuming  $t \ll R_i$ , yields

$$K = -\frac{\pi M_s H_0 L}{R_i} t. \quad (6)$$

It can be seen that  $K$  provides a net restoring force. Aside from a small difference in the constant factor this relationship recovers the result of Bottenberg [2] and the ratio of spring constants is given by

$$\frac{K_i}{K} = \frac{R_0}{t}. \quad (7)$$

Always  $R_0 \gg t$ , so it is seen that the restoring force with ferrofluid present only in the inner gap is predicted to be greatly enhanced compared to that for filling both the inner and the outer gap [4].

### 3. Measurements of voice coil centering

An apparatus was devised to measure radial force versus displacement; the results are shown in figure 2. The apparatus in these tests contained a central magnet inside a U-shaped permeable piece. Parameter values are (APG 836 ferrofluid):  $M_s = 0.022$  T,  $B_0 = 0.9$  T,  $R_i = 12.75$  mm,  $R_o = 12.25$  mm,  $L = 0.0022$  m. From equation (4) the predicted spring constant with only the inner gap filled is  $K' = 1.16 \times 10^{-2}$  g  $\mu\text{m}^{-1}$ . Figure 2 with fill ratio  $f = 1$  shows the prediction for the initial slope compared to experiment. The voice coil thickness was  $t = 0.3$  mm, so from equation (7) the ratio  $K_i/K = 408$ . The measured ratio is much smaller but significant. The variance is believed to be due to nonideal distribution of the field.

Tests in which only the outer gap was filled with ferrofluid resulted in spontaneous anti-centering of the voice coil, bringing it into contact with the outer wall in agreement with theory.

### 4. Description of the splashing phenomenon

A shock test apparatus is used in these studies in which a fixture is dropped from a known height, slides down vertical rails and impacts face down on a hard surface. The fixture contains a magnetic circuit having an annular gap that is filled with ferrofluid. The acceleration at impact is measured and the free surface of the ferrofluid photographed with a high speed video camera (9000 frames  $\text{s}^{-1}$ ). Acceleration peaks are as high as 1000  $g$  at the highest experimental drop heights. The duration of the acceleration interval is experimentally invariant of drop height, consistent with a simple magnetic mass–magnetic spring dynamic analysis and equals 1 ms.

From the videos it is seen that prior to impact the ferrofluid is confined to the gap space. Following impact the ferrofluid continues to move downward tending to escape from the fixture as a plug. The fluid is subsequently drawn back into the gap by the gradient magnetic fringe field. Modeled as a damped spring–mass system, the impact process establishes a

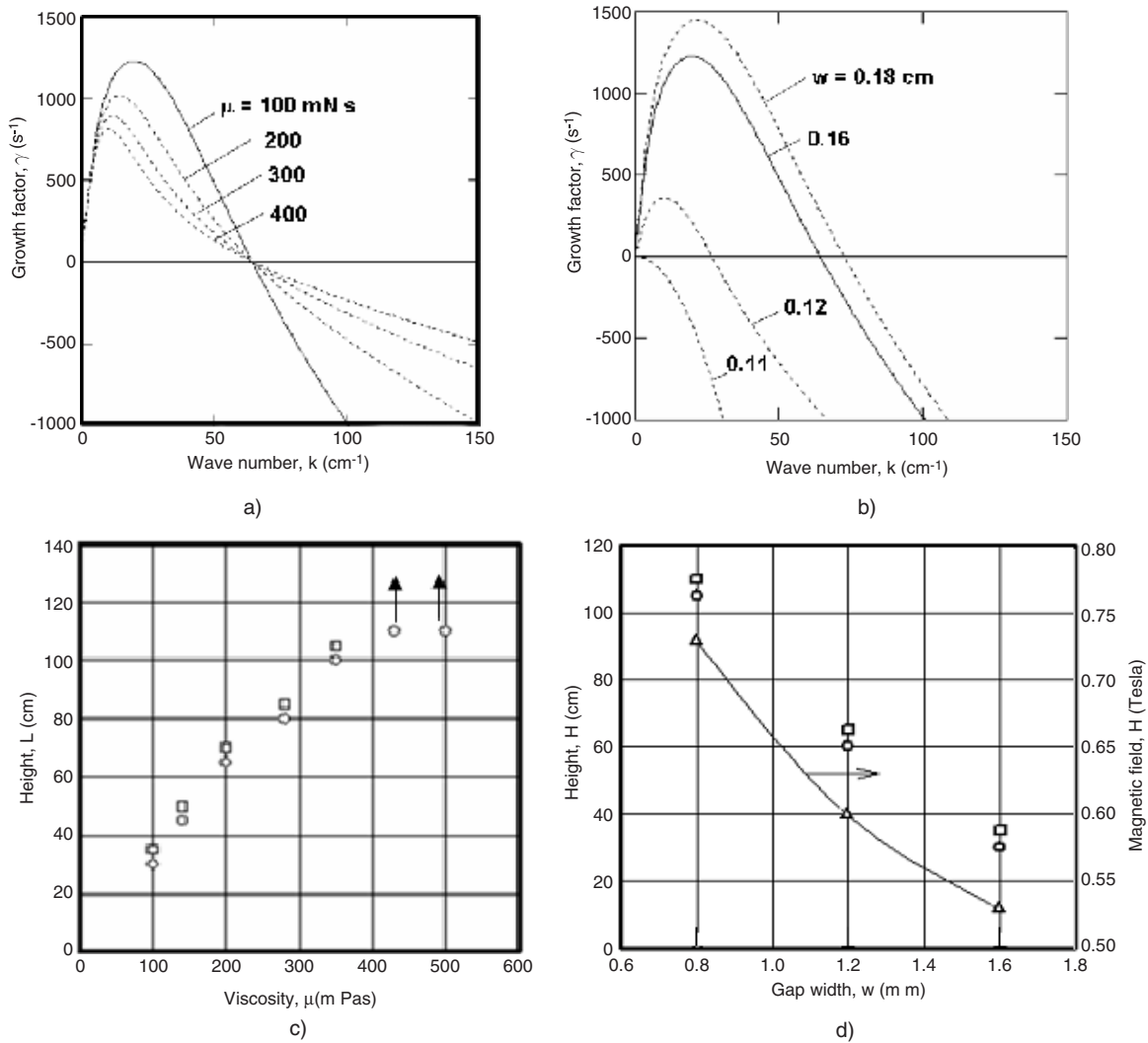


**Figure 3.** Theoretical and experimental dependences of the shock instability on the ferrofluid viscosity and gap width.  $H = 50$  cm in the Rayleigh–Taylor computations. See the text for other reference parameter values. (a) Predicted viscosity influence. (b) Predicted gap width influence. (c) Experimental height versus viscosity. (d) Experimental height versus viscosity. In (c) and (d) circles denote no splash; squares denote splash.

positive acceleration directed from the less dense medium (air) towards the more dense medium (ferrofluid), the requirement for onset of usual Rayleigh–Taylor instability [5]. Peak adverse acceleration tends to occur at the moment when the ferrofluid is maximally displaced and begins to reverse its velocity. The unstable ferrofluid interface may subsequently pinch off into droplets as seen in experiments [6].

### 5. Rayleigh–Taylor instability analysis

The analysis can define conditions for the initial growth rate of surface perturbations. The dispersion relationship for dependence of the growth factor  $\gamma$  on perturbation wavenumber  $k$  is formulated as

$$\gamma^2 + 2 \frac{k^2 \mu}{\rho} \gamma - \frac{ak}{\coth(kL)} \left( 1 - \frac{k^2}{k_0^2} - N \right) = 0 \quad (8)$$

with the growth factor  $\gamma$  defined by

$$z = \hat{z}_0 \operatorname{Re} \left[ \exp(\gamma t) \cos(ks) \right] \quad (9)$$

where  $\operatorname{Re}$  denotes real part,  $\hat{z}_0$  is the amplitude of the interfacial perturbation,  $t$  time,  $s$  distance along the mean gap perimeter,  $\sigma$  interfacial tension,  $a$  acceleration,  $L$  layer thickness,  $\mu$  coefficient of viscosity,  $\rho$  mass density,  $k_0 = (\rho a / \sigma)^{1/2}$  the Taylor wavenumber,  $\sigma$  the interfacial tension,  $N = (M / \rho a) dH / dz \approx M H_m / \rho a w$  the ratio of magnetic to accelerative body force, and  $H_m$  the maximum field in the gap of width  $w$ . The viscous term of equation (8) is that of Mikaelian [7]<sup>4</sup>, while the gradient field term of  $N$  was proposed by Zelazo and Melcher [8]. A positive value of  $\gamma$  represents instability, i.e., deviations from a flat interface grow with time.

<sup>4</sup> Note that the second line above equation (24) omits the factor 2 of the term  $X^2 Y$ ; the corrected equation (24) results in much closer agreement of the approximate result with the analytic result in figure 2.

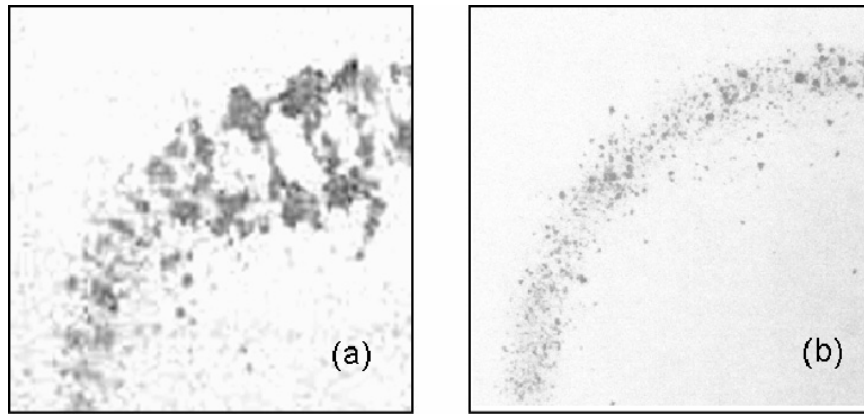


**Figure 4.** Splash patterns illustrating aspects of the Rayleigh–Taylor instability. (a) Peak acceleration 640 g; time on shelf: four days at fill fraction 1.2; wave crests are evident. (b) Peak acceleration 704 g; tested at time of filling with fill fraction 1.0; only tiny drops are seen.

*Reference physical data corresponding to ferrofluid APG810*

Viscosity coefficient: 100 m Pa s (100 cP)

Mass density: 940 kg m<sup>-3</sup> (0.940 g cm<sup>-3</sup>)

Surface tension: 0.032 N m<sup>-1</sup> (32 dyn cm<sup>-1</sup>)

Saturation magnetization: 0.011 T (ferric induction,  $B - H = 110$  G).

*Reference system parameters*

Drop height: 0.50 m (50 cm)

Magnetic field in gap: 477 500 A m<sup>-1</sup> (6000 Oe)

Gap width: 0.0016 m (0.16 cm)

Gap length: 0.0022 m (0.22 cm)

Gap outer circumference: 0.099 m (9.9 cm)

Fill fraction: 1.

Figure 2 on the right illustrates computed locations of ferrofluid boundaries with  $f = 1$ . It can be seen that end effects are significant for the short wetted length of the voice coil and hence may affect the accuracy of the predictions.

Figures 3(a) and (b) illustrate the influence of viscosity and gap width on the stability of the ferrofluid interface. The vertical axis denotes the value of the growth factor  $\gamma$ , and the horizontal axis denotes the value of the perturbation wavenumber. The crossover value of stability corresponds to  $\gamma = 0$ , with  $k_0$  the corresponding wavenumber. In the unstable range of wavenumbers ( $k < k_0$ ) a peak value of  $\gamma$  corresponds to the wavenumber  $k_m$  of fastest growth.

In figure 3(a) it can be seen that although  $k_0$  is invariant with viscosity, increasing the viscosity decreases the growth rate. This is beneficial as a sufficiently small growth rate over a limited amount of time can prevent a splash loss of the ferrofluid. From figure 3(b), it is seen that a modest reduction of the gap width to  $w = 0.11$  cm achieves incipient stability over the total range of wavenumbers. This results from generating a larger magnetic field gradient at the interface.

## 6. Experimental splash data

The trends indicated in figures 3(a) and (b) are confirmed by the data of figures 3(c) and (d), respectively. These figures plot experimental values of the drop height for the onset of splash. In figure 3(b) the acceleration is assumed constant throughout at  $a = 500$  cm s<sup>-2</sup>.

Ferrofluid splash is collected on a flat sheet of paper located 6.5 mm below the test fixture at impact; see figure 4. When splash occurs, the ferrofluid emanates from all around the gap, at times with a characteristic spacing between radial wave crests; see figure 4(a). This test was made four days after the ferrofluid was injected. By definition, the wavelength  $\lambda$  of the Rayleigh–Taylor instability is related to the wavenumber by  $\lambda = 2\pi/k$ . The wavelength of maximum growth for the reference case is 0.32 cm, corresponding to  $k = k_{\text{peak}} = 19.5$  radian cm<sup>-1</sup>. The splash pattern has  $\sim 48$  peaks around the periphery of radius  $R_0 = 12.25$  cm, yielding  $\lambda \sim 0.16$  cm. Thus, the predicted and observed wavelengths are in the same league. In figure 4(b) it appears that the initial instability producing wave crests as in figure 4(a) subsequently underwent secondary instability resulting in the production of a spray.

## 7. Conclusion

A method for achieving enhanced voice coil centering forces was validated experimentally and theoretically with comparisons made of filling both gaps, filling only the inner gap, and filling only the outer gap. It was also concluded that Rayleigh–Taylor instability in the gradient magnetic field is the mechanism of ferrofluid splash loss when it occurs. Although the experimental spacing of the ejected droplets can at times be predicted from the theory, the relationship for onset of splashing to drop height is elusive, as the magnitude of initial perturbations on the interface is unknown. However, the instability theory provides clear directional guidance for the alleviation or prevention of splashing under given circumstances. It can be said that the onset of instability predicted by the theory provides a lower bound on maximum safe drop height.

## Acknowledgment

The authors thank Professor Seiichi Sudo of Akito Prefectural University for making the high speed camera videos.

## References

- [1] Raj K 1996 Magnetic fluids and devices: a commercial survey *Magnetic Fluids and Applications Handbook* ed B Berkovsky and V Bashtovoi (New York: Begell House) chapter 5, pp 657–751
- [2] Bottenberg W, Melillo L and Raj K 1980 The dependence of loudspeaker design parameters on the properties of magnetic fluids *J. Audio Eng. Soc.* **28** 17
- [3] Rosensweig R E 1985 *Ferrohydrodynamics* (New York: Cambridge University Press) (1997) (New York: Dover) (reprinted with minor corrections and updated)
- [4] Tsuda S and Rosensweig R E, Ferrofluid centered voice coil speaker, patent applied
- [5] Taylor G I 1950 The instability of liquid surfaces when accelerated in a direction perpendicular to their planes *Proc. R. Soc. A* **201** 192–6
- [6] See images at <http://www.ame.arizona.edu/research/fluidlab/rayleigh.html>
- [7] Mikaelian K O 1996 Rayleigh–Taylor instability in finite-thickness fluids with viscosity and surface tension *Phys. Rev. E* **54** 3676
- [8] Zelazo R E and Melcher J R 1969 Dynamics and stability of ferrofluids: surface interactions *J. Fluid Mech.* **39** 1